LER-LHC INJECTOR WORKSHOP SUMMARY AND SUPER-FERRIC FAST CYCLING INJECTOR IN THE SPS TUNNEL

Giorgio Ambrosio, Steven Hays, Yuenian Huang, John Johnstone, Vadim Kashikhin, James MacLachlan, Nikolai Mokhov, Henryk Piekarz, Tanaji Sen, and Vladimir Shiltsev, FNAL, Batavia, IL 60510, USA
Gijsbert de Rijk and Lucio Rossi, CERN, Geneva, Switzerland

Abstract

A Workshop on Low Energy Ring (LER) in the LHC tunnel as main injector was convened at CERN on October 11-12, 2006. We present the outline of the LER based on the presentations, and respond to the raised questions and discussions including the post-workshop studies. We also outline the possibility of using the LER accelerator technologies for the fast cycling injector accelerator in the SPS tunnel (SF-SPS).

1 MOTIVATION

A primary goal for the LER (Low Energy Ring) injector accelerator is to inject 1.5 TeV proton beams into the LHC, instead of the current injection scheme with 0.45 TeV beams from the SPS. At this new energy, the field harmonics [1] of the LHC magnets are sufficiently satisfactory to prevent the luminosity losses expected to appear when applying the transfer of the 0.45 TeV SPS beams. In addition, a feasibility study of batch slip stacking in the LER has been undertaken with a goal of increasing in this way the LHC luminosity by up to a factor of 4. A combined luminosity increase may, therefore, be in the range of an order of magnitude. In the long term, the LER injector accelerator would greatly facilitate the implementation of a machine, which doubles the LHC energy (DLHC).

2 LAYOUT OF THE ACCELERATOR AND THE SPS-LER-LHC BEAM TRANSFER

The LER accelerator will be installed inside the LHC tunnel. This accelerator would accept 0.45 TeV proton beams from the SPS through the existing TI2 and TI8 transfer lines, and then accelerate these beams to 1.5 TeV, so as to better match the beam acceptance of the LHC magnets. A preliminary outline of the LER was presented in [2]. The LER accelerator would be based on super-ferric, combined function magnets. These magnets were originally proposed for the VLHC Stage 1, a p-p collider in the US [3]. A basic property is that they require only minimal space in the accelerator tunnel. The magnet and its supporting systems (conductors, power supply, current leads, etc.) were recently successfully tested at Fermilab [4-8].

In the new LHC beam injection scheme, the proton bunch stacking and the formation of the full intensity beam is performed in the LER ring. Once the stacking of the clock-wise and the counter-clock 0.45 TeV beams in LER is completed, the beams are accelerated to 1.5 TeV. At this top energy, the beam is passed into the entire LHC ring using a single transfer mode through one of the transfer lines. For this single transfer, only one set of the LER transfer line magnets is to be ramped down. The ramping down has to be done in a time period determined by the time interval between the tail and the head of the beam train. The other transfer lines (2 x 2 transfer lines in total) are switched off when the hole in the beam train passes. This idea of LER to LHC beam transfer is illustrated in Figure 1

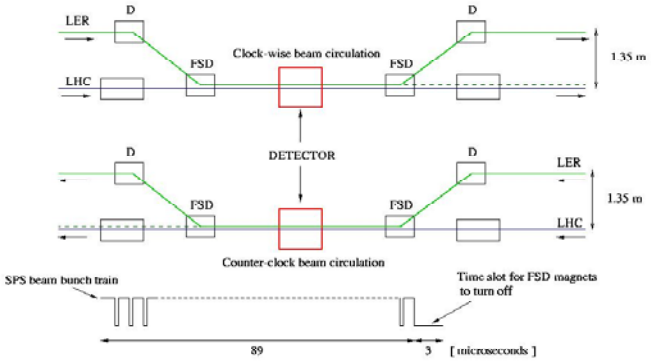

Figure 1. Principle of the proposed LER-LHC beam transfer method

The minimum allowable vertical separation between the LER and LHC rings is about 135 cm. In the IR regions, where the detectors reside, the total length of the straight sections is about 528 m. The available space, on each side of the detectors, at the LHC ring level that could be used for inserting the LER-LHC transfer-line magnets totals only about 80 m. This situation poses a great challenge for the transfer of the 1.5 TeV beam between the two rings. A possible conceptual LER-LHC transfer line design and arrangement of the transfer line magnets in the IR1 and IR5 regions are discussed in Chapter 7. The proposed conceptual LER-LHC injection scheme together with the LER ring arrangement is shown in Figure 2.

A set of fast switching magnets placed in the front straight sections of the IR2 (ALICE detector) and IR8 (LHCb detector) performs the beam transfer into the LHC

ring. We assume that in the high-luminosity LHC operations these detectors will not be used, but the proposed scheme will allow using these detectors any time as the LHC can be reverted to its current-type operation.

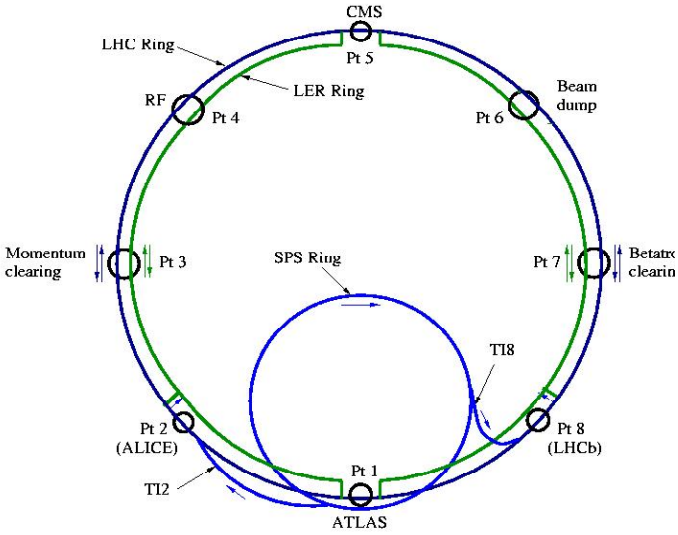

Figure 2. Conceptual arrangement of the LER-LHC injection scheme

The beam from the TI2 transfer line enters the LHC ring at the short straight section just in front of IR2. It travels through IR2, passes the IR3 and IR4 areas, and is transferred into the LHC beam pipe only in IR5 where it passes through the CMS detector. It is again bumped into LER passing through the IR6, IR7 and IR8, and it re-enters the LHC beam pipe at IR1 (ATLAS). Immediately after IR1 it is bumped back into the LER ring, and will stay there until reaching IR5. The beam from TI8 has the same path in LHC/LER as the TI2 one, except that it enters the LER ring right after IR8 and it travels in counter-clock direction. The LER has its own momentum and betatron clearing at IR3 and IR7, respectively as well as its own RF system at IR4 and the beam dump system at IR6.

3 THE VLHC STAGE 1 MAIN ARC MAGNET AND ITS APPLICATION TO LER

3.1 Main arc magnet design considerations

A conceptual view of the VLHC Stage 1 main arc dipole magnet is shown in Figure 3. The magnet features two pole gaps between the top and the bottom half-cores. The magnetic field is induced by a current of up to 100 kA from a single transmission line conductor located in the centre of the half-core assembly. The field in the pole gaps is entirely shaped by the iron. The magnet is a combined function gradient dipole with two half-cell versions, focusing and de-focusing, which are placed alternating along the accelerator ring. The magnet pole gap is 20 mm high, and the beam pipe is elliptical with an effective vacuum space of 18 mm (v) and 28 mm (h).

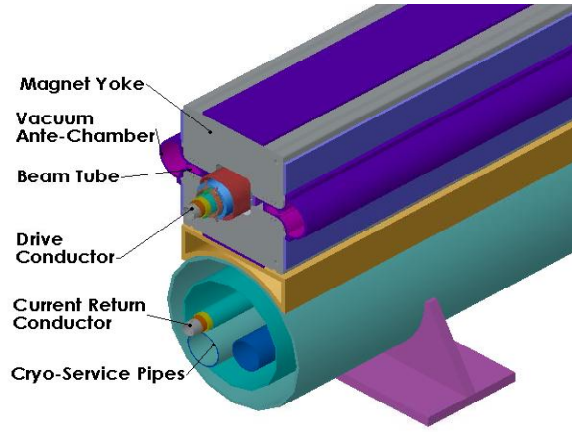

Figure 3. The VLHC Stage 1 magnet conceptual view

The characteristic measured dipole strength versus current is shown in Figure 4.

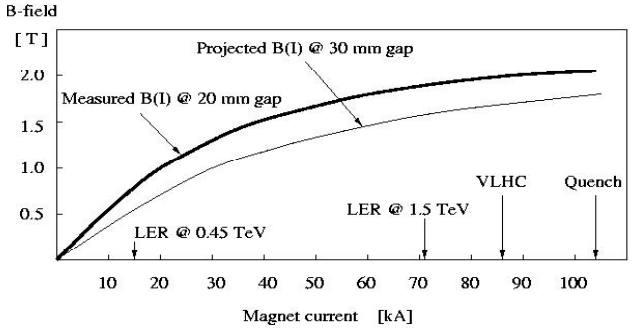

Figure 4. Measured dipole field, and projected B(I) response for a 30 mm LER magnet gap

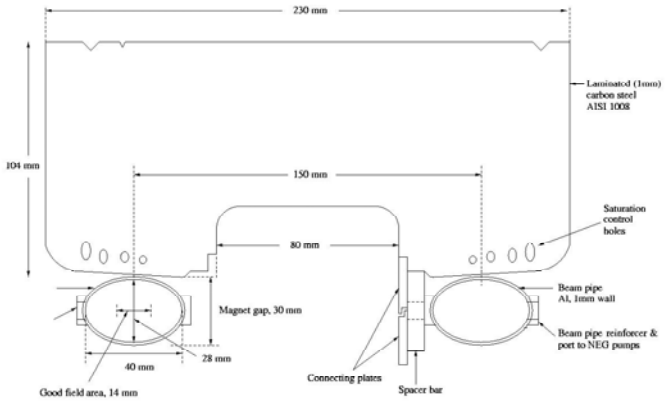

Figure 5. Proposed new lamination design for the LER main arc magnet

As demonstrated in Chapter 6, the required dipole field for the LER main arc magnet is 1.6 T for a 1.5 TeV beam. This leads to a strong reduction of magnet current (45 kA), and very importantly the magnet operations are moved nearly out of the saturation zone. We take advantage of this situation and propose to widen the magnet gap to 30 mm. This new gap will help to reduce beam impedance effects (Chapter 7.1) as well as it will facilitate implementation of bunch coalescing techniques (Chapter 7.2) with LER. The lower field also allows reducing the vertical size of the magnet core lamination to just contain the 1.6 T magnetic flux. A new possible lamination design is shown in Figure 5. The beam pipes are enlarged to 28 mm (v) and 40 mm (h). New simulations are needed, however, to determine the definitive dimensions of the lamination.

3.2 The LER main arc magnet conductor

The LER main-arc dipole magnets will be powered with a single transmission line conductor [3] using a single power supply [5] and a single set of current leads [6] as shown in Figure 6.

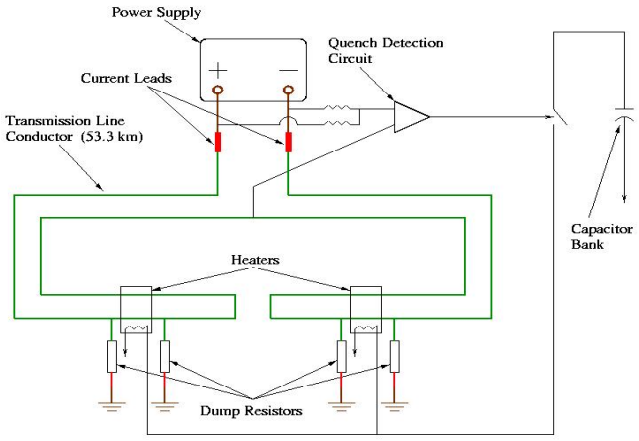

Figure 6. Arrangement of the LER transmission line conductor

The drive conductor loops through half of the accelerator circle, turns 180º, runs as return conductor the full circle, turns again 180º and then excites the other half of the accelerator magnets. This makes the continuing length of the conductor ~ 53.3 km. As the currents in the overlapping conductors run in opposite directions, the magnetic fringe field of the LER magnet string is strongly suppressed at far distances, and the magnetic field in the space between the two neighboring magnets is totally suppressed.

Both the drive and the return conductors must bypass the detector areas. In this area the drive and the return conductors are separated vertically by 28 cm, and the cryostat pipe enclosing both of them is only 36 cm in diameter. This indicates the space, which is needed in the area behind the detectors for the installation of the bypass conductor lines.

The conductor lines must be equipped with quench detection and protection circuits. A conceptual design of the quench detection and protection system for the VLHC is presented in [9]. With a magnet inductance of 3 μH/m, the total inductance per LER ring is ~ 80 mH, and the stored magnetic energy per ring at 45 kA current is ~ 53.3 MJ. In the VLHC design report [3] it was shown that only one quench detection/protection circuit per 20 km of the conductor length is required. Scaling from that study we project that with one quench detection and protection system for the LER ring, the helium peak temperature and pressure will rise up to ~ 65 K and ~ 9 bar.

3.3 The LER main arc magnet power supply

The original concept for the VLHC transmission line magnet system was to be a p-p collider that required extended operation at 100 kA. The magnet system would be loaded to the 3 kA level and ramp to the 100 kA level in 100 s. To provide the ramping voltage, a 400 V pulsed duty supply was to be constructed and a power supply of lower voltage would be used to hold the current. To provide the DC current, a switcher power supply that operates at 4.5 V and 100 kA was developed and successfully tested [5].

The LER magnet system is intended to be an injector used in support of the LHC. This means that this magnet system will only pulse for 20 minutes at the time of reloading the LHC. All magnet systems (quad, trim, fast pulsing and kicker charging supplies) will need to track this ramp cycle, illustrated in Figure 7.

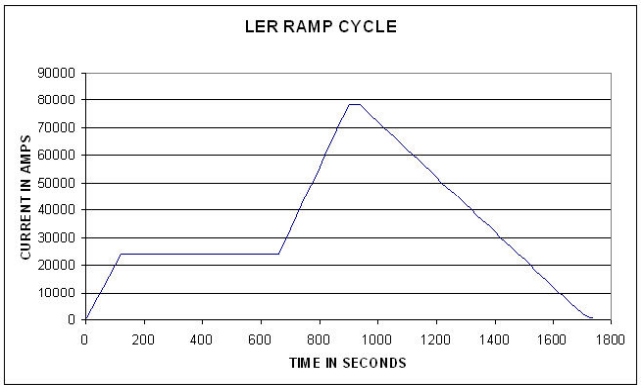

Figure 7. A characteristic current supply ramping scheme for the LER magnets

The support magnet systems are expected to operate from a 400 V DC bus and be constructed using standard DC-DC converter designs. The abort kicker magnets charging power supply system are expected to be CAP charging power supplies and be of present conventional kicker system design

A ramping power supply will need to be constructed to provide +20 V / -18 V @ 72 kA. This voltage assumes that a superconducting dump switch is designed and

installed into the system to avoid the 2 V - 3 V drop of each conventional switch. The construction of this supply is expected to extent the present FNAL designs using parallel power supplies summed through filter chokes to provide this high current. A reasonable design for this supply would be using four 20 kA supplies (Figure 8) in parallel with a peak feeder loading 1.1 MVA..

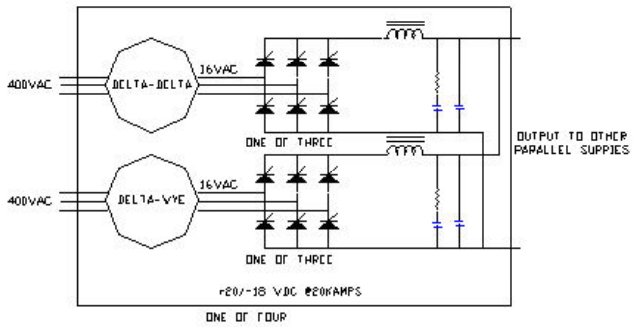

Figure 8. A design for a 20 kA supply

Each of the 20 kA supplies is constructed using two 10 kA bridges supplied from one Delta-Delta and one Delta-WYE transformer, summed together through two chokes and then filtered. Using FNAL design criteria the bridges would be constructed for full current, 10 kA each while the transformers need only be rated for the half the power between the RMS and Peak power values. We recommend that the RMS value should be the injection value rather than zero thus allowing for LER to sit at injection level for an extended period of time, if needed. Therefore the RMS value should be 315 kVA and the peak value 1100 kVA, and then the transformers would need to be rated for 834 kVA (210 kVA each pair) and braced for the full pulsed current at the output and peak loading at 1.1 MVA.

This power supply design builds on the Main Injector dipole power supply system [10], which uses 10 kA SCR bridges in parallel. At the FNAL Magnet Test (MTF) a 30 KA system exists, that uses 6 power supplies paralleled through chokes and bus-work. The current feedback for the MTF system is provided by summing 5 kA DCCT's for at the output of the summing chokes but each 12 pulse supply is used as a regulated source. A 418 V, 10 kA DC supply was constructed under a development project for the Main Injector power supply bridges and could be used to further detail the design of this power supply. The Main Injector power supply bridges are constructed with three parallel SCRs and use a cable bus system to the transformer to assist in current balance and sharing. This magnet power supply system also can operate in a mode where the transformers are pulsed above the RMS rating. It will need a harmonic filter installed on the main feeders to control the pulsed current and the power factor. The design elements for this power supply are available now and need to be only organized into a system. It is very important to construct the power leads to be as close as possible to the power supply to limit the difficulty of building a high current distribution bus

3.4 The LER main arc magnet cryogenic support

The cryogenic heat load of the main arc magnet is generated predominantly from the conductor support inside the cryostat. This support is made of Ultem™ rings

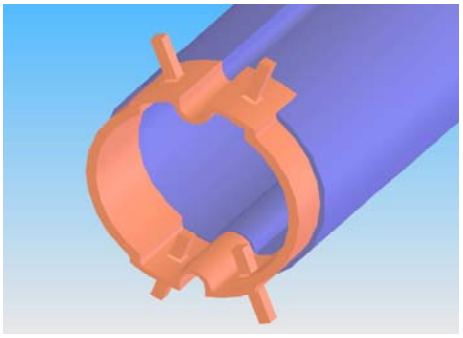

Figure 9. Cryogenic support ring and shield for the LER main arc magnet conductor

with 4 pegs every 0.5 m as shown in Figure 9. The inner pegs hold the conductor, while the outer pegs hold the cryostat vacuum pipe. The thermal shield at 50 K is also attached to the rings through an aluminum pipe. Both the shield and the conductor are wrapped with in total 60 layers of the MLI super-insulation. The heat loads due to main arc magnet conductor are summarized in Table 1. There are eight arcs in the LHC each with corresponding cryogenic support of an 18 kW cryo-plant. The total LER main arc magnet conductor heat load is ~ 4 kW, small enough to be supported from the existing LHC cryogenic system which consists of 8 refrigerators, each of 18 kW power at 4.5 K, and 600 kW power at pre-cooler.

Table 1. The LER main arc magnet conductor heat load

	4.5 K – 6.0 K level	50 K - 75 K level
Mechanical supports (mW/m)	53	670
Superinsulation, MLI (mW/m)	15	864
Beam loss (mW/m)	2	1
Splice (mW/m)	7	-
Total conductor heat load (mW/m)	77	1535
Main arc conductor heat load (kW) (LER drive & return conductors, ~ 53.4 km)	4.1	82

3.5 Arrangement of the LER magnet ring in the LHC tunnel

The inspection of the LHC accelerator tunnel leaves only one possibility for the location of the LER magnet, and that is in the space above the LHC magnet as shown in Figure 10. The return conductor of the LER magnet is placed in the space above this magnet thus minimizing a

potential effect of LER magnet fringe field on the LHC operation. Fringe field simulations on the LER magnet are needed to determine if magnetic shielding is needed to protect the LHC.

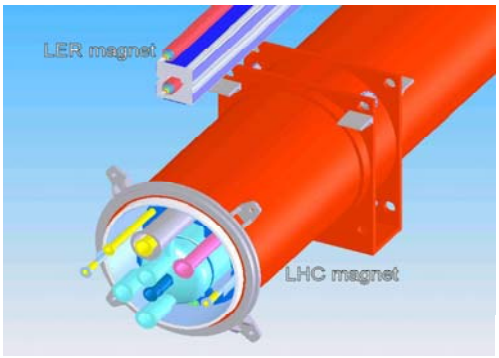

Figure 10. Arrangement of the LER and LHC magnets in the tunnel

The magnet will be supported from two crossing I-beams fastened to the top and the side of the concrete wall of the tunnel. The I-beam spacing is to be determined by an engineering analysis of the strength required to support the magnet weight of 500 kg/m. There are, however, some obstacles for the LER magnets, typically located in straight sections IR1 and IR8. The main obstacles are: (1) the LHC magnet power cables on the distribution boxes which are fed to the magnet top (~ 10 m long space at each side of each IR is used), (2) helium feeds from the top or from the sides at all IRs (~ 15 m space), and the power cables for the accelerating cavities at IR4 (~ 50 m). Although a re-arrangement or a bypass of these obstacles may not be easy, it does not appear to be un-surmountable task.

3.6 LER main arc magnets and correctors count

As thoroughly analyzed in [3], the main arc magnets, which are of combined function design, require a set of correctors on every half-cell. These corrector magnets can be normal conducting.

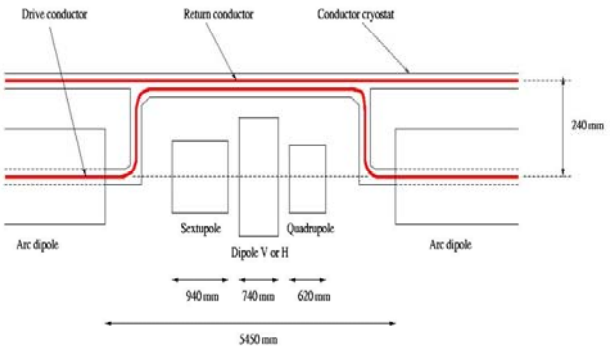

Figure 11. Arrangement of the main arc dipole corrector magnets

There is about 5.5 m free space between half-cells of main arc magnets. The correctors use this space where the drive conductor will be moved up by 230 mm, to be next to the return conductor as indicated in Figure 11. Each corrector magnet set consists of a sextupole, a quadrupole and interchangeably a vertical or horizontal dipole for every half-cell. A summary of the LER magnet count is shown in Table 2.

Table 2. The LER main arc magnet count

Magnet type	Field	Length [m]	Count
Main dipole	1.6 T	12	1640
Dispersion suppresser	1.6 T	8	128
Dipole corrector (H or V)	0.8 T	0.5	410
Quadrupole corrector	20 T/m	0.5	410
Sextupole corrector	1400 T/m^2	0.8	410

4 LER-LHC TRANSFER LINE MAGNETS

4.1 Conceptual arrangement of the LER-LHC transfer line

Beam transfer from the LER ring into the LHC ring is the most challenging task of the LER proposal that needs to be very seriously dealt with. The vertical separation of the LER and LHC rings can be made to be 135 cm. This means that the 1.5 TeV beam needs to be bent down (or up) out of the LER (or LHC) ring, transported, and then bent into the LHC (or LER) ring over a vertical distance of 135 cm. A free drift space spans only 70.5 m mostly between D1 and Q5. The basic concept of the LER-LHC beam transfer is shown in Figure 12, and the beam line design is presented in Chapter 7. There are two sets of bending magnets. The first one lifts the beam over the D2 and the second one puts the beam at 1.35 m above the LHC ring. The 1.35 m level is the nominal level of the LER ring.

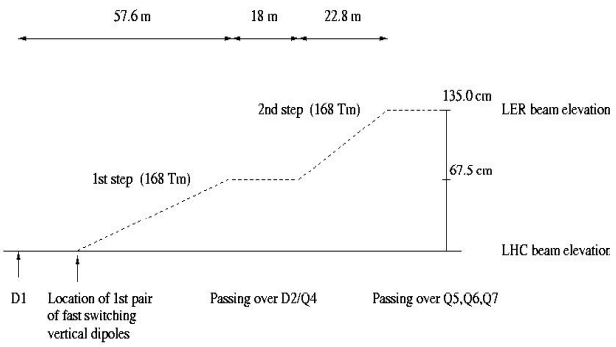

Figure. 12. The basic concept of the LER to LHC beam transfer

In the horizontal plane the clock-wise and counter-clock-wise turning LHC beams have no separation at D1, but they are separated by 194 mm at D2. The first LER magnet pair of the first vertical bend section must be

placed at a location where the clock-wise turning and counter-clock-wise turning beams are separated enough to allow for operating these close neighbouring magnets with a good magnetic field quality. A preliminary magnetic design suggested that a 110 mm - 130 mm beam separation should be sufficient. However, with the present LHC design such a beam separation is only in achieved in about 2/3 of the D1–D2 distance of 86.6 m, making it impossible to accomplish the two first LER beam transfer bends before the D2 magnet. The required horizontal LHC beam separation can be only achieved in a shorter distance from D1 by redesigning the D1 and D2 LHC dipole system. A conceptual proposal of the new D1 and D2 dipole arrangement together with an outline of the LER-LHC transfer line magnets is shown in Figure 13.

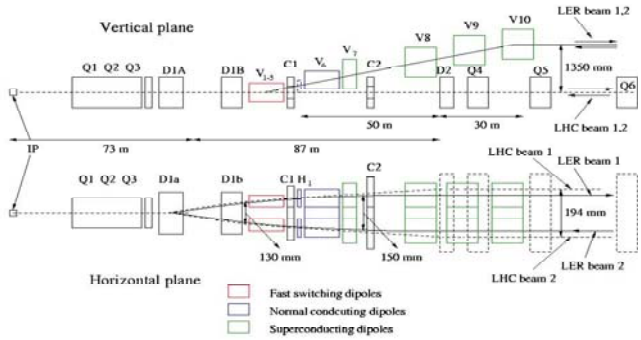

Figure 13. Conceptual arrangement of magnets in the LER-LHC transfer lines

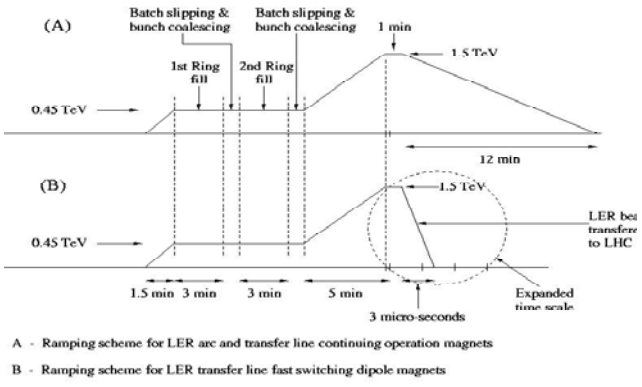

Figure 14. Timing sequence for ramping LER and beam transfer to LHC

The LHC D1 dipole magnet is split into two parts, D1a and D1b, with a beam drift space of about 12.5 m between them. Assuming that a magnetic field of 8 T is feasible for the new D1 magnets, this drift space will allow the creation of a separation of the clock-wise and counter-clock-wise turning beams by up to 130 mm at the exit of D1b, sufficient for the installation of the V1-5 fast switching magnets. The integrated field strength of the V1-5 magnets allow for the LHC and LER beam pipe separation at the end of their path. All the following sets of transfer line magnets are well above the nominal LHC beam line, and so they can be in a continuing mode of operation, as their magnetic fields are not interfering with LHC beams.

In order to understand the choice and arrangement of magnets in the first bending set we must look at the timing sequence of the SPS-LER-LHC beam transfer scheme. This is schematically indicated in Figure 14. When the SPS is ready for beam transfer, all LER magnets, including those in the transfer lines, are ramped up to the required fields for the 0.45 TeV beam. A ramping time of 90 s is characteristic of the main arc LER magnets. The stacking of the first LER beam begins and it lasts for about 3 min. Then the stacking of the 2nd LER beam begins and lasts for about 3 min as well. As soon as the beam stacking is complete the LER magnets ramp to 1.5 TeV. The 1.5 TeV beams may circulate for 1 min - 2 min, or so, to allow e.g. for beam tuning if needed, and then the fast switching LER-LHC transfer line magnets are turned off, forcing the beams to circulate from now on in the LHC ring only. At this point all remaining LER magnets are ramped down. The operation of the fast switching magnets is more complicated, however, due to the fact that for each beam the magnets on the opposite sides of the IR must work in tandem. This is illustrated in Figure 15.

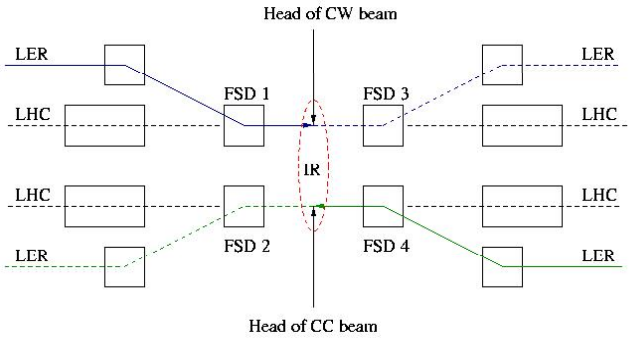

Figure 15. Timing relation between neighboring fast switching magnets

When the tails of the LER beams pass magnets FSD3 and FSD2, these magnets have 3 μs to be completely turned off before the heads of the LER bunch trains will reach again this position. But the FSD1 and FSD4 magnets must operate for an additional 86 μs until the entire LER beams are transferred into the LHC ring. So, the FSD magnets on the same side of the IR have opposite timing sequences during the beam transfer. This means that the fringe fields of these magnets must not extend into the beam gaps of their counter-parts in the neighbouring accelerator ring.

4.2 Fast switching dipoles for the LER-LHC transfer lines

4.2.1 Magnetic design considerations

The fast switching magnets must be powered with a single conductor in order to minimize the inductance. Typically, such magnets can be designed with an inductance of ~ 1 μH for a length of ~ 1 m. In order to minimize the required current for the 1.5 T field in the 40 mm magnet gap, we designed a magnetic core that "boosts" the gap field by as much as factor 2, and so the required power supply current is ~ 50 kA. With a 1 μH magnet inductance, the peak voltage drop with a 3 μs turn-off time is then ~ 27 kV, plausibly manageable.

There are two options for the magnetic design: (1) based on parallel plate conductors, and (2) based on cosine Θ shaped conductors. We selected the first one as a primary choice due to its simple mechanical structure and the much lower Eddie current effects. The core is made of Fe3%Si, 100 μm thick laminations, to meet the criteria for operating in a ~ 3 μsec time range. The projected B(I) response and laminated magnetic core design are shown in Figure 16. B-field to current response is linear up to 1.5 T, the field range of the fast switching magnets.

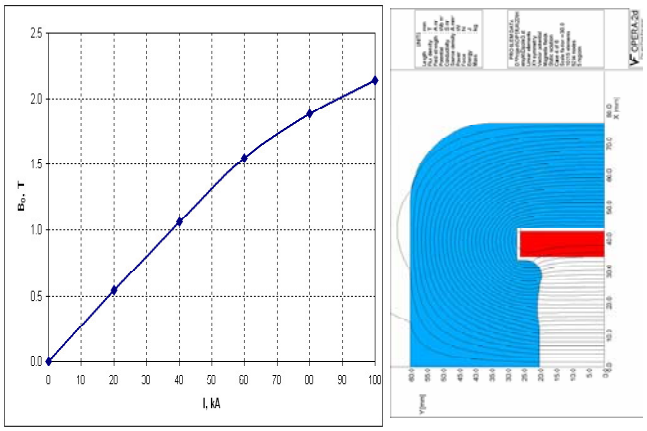

Figure 16. A projected response of B(I) for a parallel plate magnet with a 40 mm gap and a magnetic core of laminated design

4.2.2 Conductor and mechanical design considerations

The cross-section area of a normal conductor for the fast switching magnet is ~ 436 mm^2. With such a small cross-section, the current induced Joule heating makes it difficult to operate with a 55 kA current for a time period of 10 min, the time needed for the LER beam stacking. The best solution for the conductor Joule heating problem is to use a superconductor. In this case the heat load is mostly due to the conductor cryogenic support but the heat generated by Eddie currents must also be considered. The Eddie currents generate an opposite sign magnetic field in the magnet gap. This, in turn, slows-down the current decay time when the magnet is switched off. This effect can be compensated at the expense of additional power (current) given to the conductor. A summary of projected Eddie current B-fields with associated heat loads for a 55 kA magnet current using conductor strand designs of NbTi, HTS-344S [3,11] as well as the OFHC copper strand of RRR = 1000 is shown in Table 3.

Table 3. Some properties of the conductors considered for FSM magnets

Conductor type	Strand cross-section	Number of strands	Operating temp.	Maximum temp.	Eddie currents			Cryogenic support heat load	Total LHe flow
					B-field	Heat	Temp.		
	[mm^2]		[K]	[K]	[T]	[J]	[K]	[W/m]	[g/s-m]
NbTi	0.42	288	5	8	0.22	0.35	0.03	0.16	0.01
HTS (344S)	0.65	264	5	20	0.002	0.03	0.003	0.16	0.01
Cu (RRR=1000)	0.65	678	5	20	2.17	34	3	30	1.5

The Eddie current effect is minimized by suppressing magnetic flux which crosses the conductor. The CERN kicker magnet [12] is a good example of a design where the Eddie current induced field distortion during the 3 μs ramp to 0.6 T field is at most 5%. The magnetic design shown in Figure 15 is consistent with the CERN design, and so we expect only minor field distortions due to Eddie currents as indicated in Table 3. As the magnetic field distortion occurs only during the gap between bunches (when one of the magnets is turned off) it will not affect the particle beam, provided that the power supply was successfully turned off and so the magnet current has fully decayed. The strength of the Eddie current B-field may have strong impact on the mechanical structure of the conductor assembly and therefore it should be minimized. As the duration of the Eddie currents is limited to an ~3 μs time period, it has only a small effect on the overall conductor heat load.

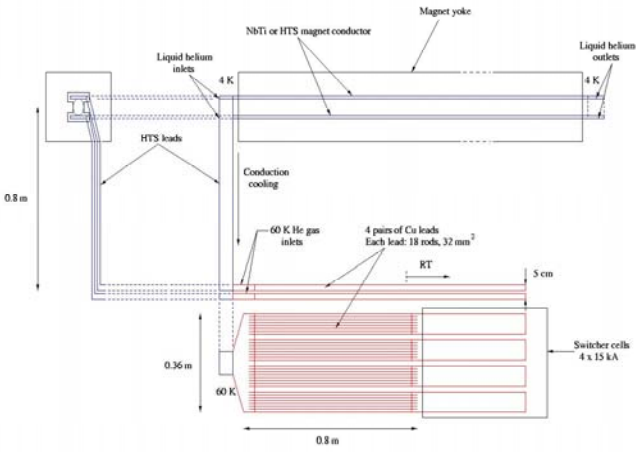

Figure 17. A conceptual design of current leads for the FSM magnet

FSM magnets using superconductors, will have their total heat load dominated by the current leads. Current leads based on HTS superconductors offer the lowest heat load, and therefore rather low liquid helium consumption as demonstrated recently in [13]. We project for the FSM

magnet current leads, operating at a current of 60 kA, that the heat load will be ~ 6 W per lead, and the total heat load for all fast switching magnets in IR1 and IR5 will be ~ 0.7 kW, which is easily supported from the existing LHC cryogenic system. A conceptual design of the FSM magnet current leads is shown in Figure 17. In this design the power connection to the magnet is made using two-step current leads. The HTS leads must have enough superconductor material to carry the current required for the magnet up to 70 K. At this temperature conventional leads will make the connection to the power supply. The liquid helium flow is used only to cool the conductors inside the magnet, and conduction cooling is used for the HTS leads. At the location where the HTS leads are spliced to the conventional Cu leads, the 60 K helium gas flow is used to provide cooling. The length of the copper leads (~ 0.8 m) is calculated so that at the connection point to the power supply they are at about room temperature. In Figure 18 two possible arrangements of NbTi and HTS-344S superconductors into conductor bars are shown.

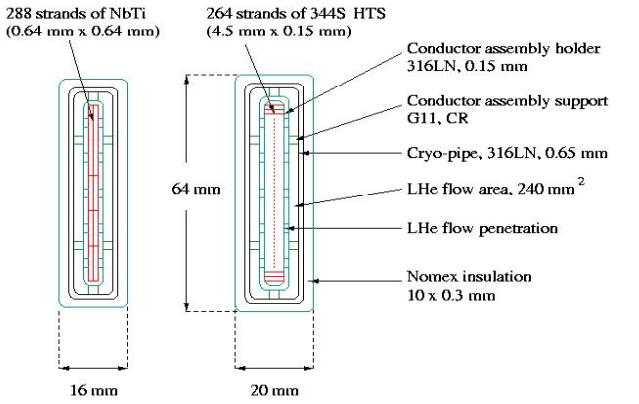

Figure 18. Arrangement of NbTi and HTS (344S) strands into a conductor bar

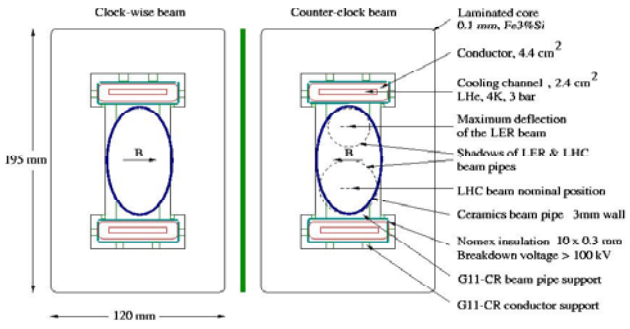

Figure 19. A conceptual arrangement of the FSM magnet pair

Each strand is electrically insulated using a polyimide tape of 0.025 mm thickness. The conductor strands are held inside a 316LN case, which is insulated for a voltage larger than 100 kV with 10 layers of 0.3 mm Nomex tape. A possible mechanical arrangement of the FSM magnet pair is shown in Figure 19. These magnets would use a ceramical beam pipe and the conductor bars will be thermally isolated from the magnetic core with help of G11-CR supports.

4.2.3 The FSM magnet list

Using the above magnetic and mechanical considerations for the FSM magnets and the transfer line design described in Chapter 6, we derive the list of transfer line magnets as shown in Table 4. The guiding principles were: (1) - not to exceed the 1.5 T B-field, and (2) - to keep the single magnet inductance under ~ 1.5 μH. This low inductance allows for keeping the peak voltage below 45 kV during the magnet turn-off time, and thus being well below the electrical insulation design limit at 100 kV.

Table 4. The FSM dipole magnet list

Magnet gap [mmxmm]	Vertical lift [mm]	Magnet length [m]	B-field [T]	Inductance [mH]	Peak voltage [kV]	Number of magnets	Number of supplies
40x40	0–5.5	1.6	1.46	1.3	40	4	4
40x50	5.5–16.2	1.4	1.46	1.5	43	3	3
40x60	16.2–27.6	1.3	1.46	1.6	46	2	2
40x70	27.6–36.6	0.9	1.46	1.3	40	2	2
40x80	36.6–46.2	0.8	1.46	1.3	40	2	2

4.2.4 Fast switching magnet power supply considerations

Turning off the magnet's supply current in a time span of 3 μs is the most challenging part of the LER transfer line proposal. A short current decay time constant must be enforced on the system. Typically, an IGCT (Integrated Gate Commutating Thyristor) device installed in-line with the magnet leads, is used for such applications. A new idea is proposed for enforcing fast magnet current decay that takes advantage of the cold environment around the magnet,. A conceptual arrangement of such a system is shown in Figure 20, and its electronics circuitry is shown in Figure 21

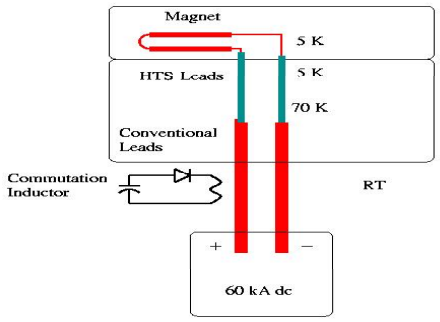

Figure 20. Conceptual arrangement of FSM magnet, current leads and pulse kicker PS

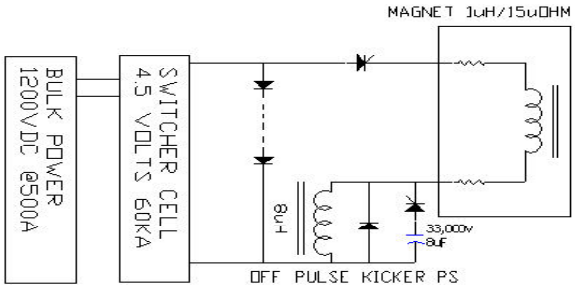

Figure 21. The FSM magnet pulse kicker power supply arrangement

This power supply system concept combines three elements of presently used superconducting magnet systems: a forced commuted dump switch, a kicker power supply and a switcher supply. One of the current leads to the magnet is instrumented with a pulsed commutation inductor (CI). This inductor will be smaller if it is situated in the cold area but it could also be in the warm area inside the high voltage tank of the kicker power supply. If installed in the cold area, an additional pulsed current lead would need to be brought out of the magnet to connect to the kicker pulser. In any case the inductance added to the system by its physical constraints will need to be minimized using either strip-line or micro-strip methods in the HTS magnet conductor leads.

In order to stop the magnet current, the CI must provide a higher impedance than that of the magnet and the common point is pulsed from a kicker style power supply to 30 kV and 50 kA for 3 μs. This increases the current in the inductor from 50 kA to 58 kA and the current in the magnet from 50 kA to zero in 3 μs. At the time the current reaches zero, the IGBT switch is turned off. This allows for zero current switching of the IGBT and helps to reduce the blocking voltage needed for the switch. To protect the switch from turning the device off at high current, a self-retrigger circuit will be installed. The superconductor may heat-up due to Eddie currents during the pulse and stop being superconducting, forcing the current to commutate into the SS substrate of the HTS conductor and in this way creating a shunt resistor. This shunt resistance increases the series resistance of the magnet, which may decrease the turn-off time. The speed of this commutation is unknown but should have little effect on the overall speed of the system.

A more detailed block diagram of the FSM magnet power supply system is shown in Figure 22. The left side of the diagram represents the switcher power supply and the output filter. This switcher supply is a subset of the holding supply, which was developed and tested for the VLHC. Due to the low inductance and the low ramp rate of the system, the output of the supply is bypassed with diodes that are used to decrease the reflected inductance to the kicker pulse which lowers the required voltage. The bypass diode will need to be located close to the magnet to minimize the stray inductance, but allowing in this way for the switcher to be located farther away from the magnet. The energy stored in the switcher power supply filter inductance is discharged at a slow rate through these diodes and the bus resistance. The IGTB is turned off at the zero current point, which then blocks the positive voltage on the bypass diodes, +18 V, and -18 V on the ring down diode across the pulsed inductor which is the result of the high current in the diodes. The 36 V would try to refill the magnet resulting in a non-zero current for the decay time of the stored energy in the inductors. Even though the IGBT is a fast turn-off device the need for voltage protection will require a ZNR and snubber cap that will prevent the switch from acting as if truly open to the magnet. The details of this protection will have to be well understood to insure that the voltage on the device is kept low during a false turn off and that the current leakage back into the magnet is at a minimum.

The kicker pulse circuit is shown on the right side of the diagram. This system uses a proven design that incorporates a solid-state turn on switch to pulse the current and the voltage. There have to be two of these switches installed in the system in a parallel arrangement. The high-speed forward conduction path of the kicker is from the kicker cup through the kicker switch on the magnet to the IGBT, and then to the bypass diode.

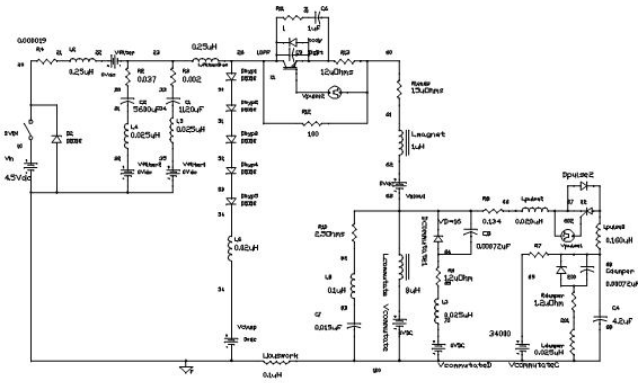

Figure 22. More detailed schematic of the FSM magnet power supply system

This current path will need to have a strip-line construction to keep the stray inductance as low as possible. When the kicker switch turns off at the end of the pulse the commutation inductor current has to switch fast into the commutation diode to minimize the re-applied voltage to the magnet and the IGBT switch. The high-speed current switching into the bypass diode, kicker diode and commutation diode will require that the diode stacks are constructed using kicker element designs.

With the physical size of the system being rather large there is little space left for the DCCT for high current feedback. Continuation of the development of cold a DCCT at a 60 kA level that could be installed on the power leads would allow to considerably reduce the space and to minimize the bus work.

The theory of operation of this system is that the kicker pulser will receive a trigger timed by the 3 μs abort gap reaching the first FSM magnet in the LER-LHC transfer line, and start taking the magnet current to zero. At the same time the drive to the switcher power supply is turned OFF and the output voltage will change from 4.5 V to - 0.55 V, using the bridge diodes as a bypass. The kicker current pulse will force to commutate the current in the magnet to zero and divert the switcher filter current into the bypass diodes. When the current in the IGBT switch is at zero, it is turned off and the magnet circuit is open. At the same time the kicker stops conducting and the commutation choke current is switched into the commutation diode.

The two elements with high current flowing will decay over 9 ms - 10 ms time, leaving the magnet with zero current. As one can see in the simulated functions of the FSM magnet power supply in Figure 23, the current is rising both in the commutation and bypass diodes and therefore a parallel path for sharing and lowering the stray inductance will be required. The current in the commutation diode has an oscillation that is the result of the current in the kicker pulse inductance, cap bank diode and the commutation inductor ringing.

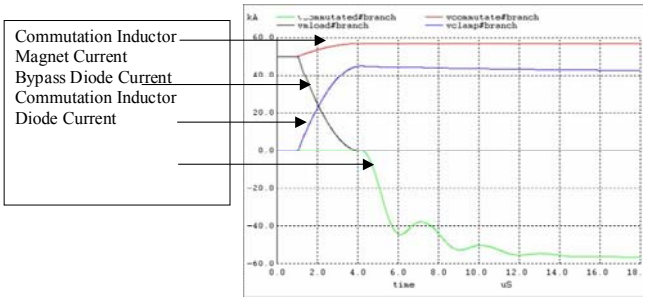

Figure 23. Simulation of currents and voltages of the FSM magnet power supply during turn-off

4.3 Other LER-LHC transfer line magnets

The last pair of fast switching dipoles, V5 (see Figure 12), separates the LER beam path from the LHC beam path by 46 mm. This separation is increased to 75 mm by allowing the beam to drift for about 4 m. The 75 mm separation is sufficiently wide to install the LHC beam pipe inside the V6 magnet core without affecting its magnetic properties. The arrangement of the first pair of the V6 magnet string with LHC beam pipes inside their cores is shown in Figure 24. When the LER beam is deflected vertically to about 115 mm, the LHC beam pipes are totally outside of the V6 magnets cores (Figure 12). As the V6 magnets carry only the LER beam, a beam pipe with a diameter of 30 mm is sufficient. This in turn, allows to increase the magnetic field to 1.95 T while keeping the magnet current at 55 kA. The entire string of V6 magnets is energized by a single power supply. The string of six V6 magnets lifts the LER beam to about 170 mm above the LHC beam path. This gives enough separation from the LHC beam path to install the V7, high-field type magnets. In order to fit the entire LER-LHC transfer line in the beam path ending before the Q5 magnet of the LHC, all V7 magnets have to operate at no less than 8 T field. The V7-type magnets are vertical bending dipoles that have shared magnetic cores.

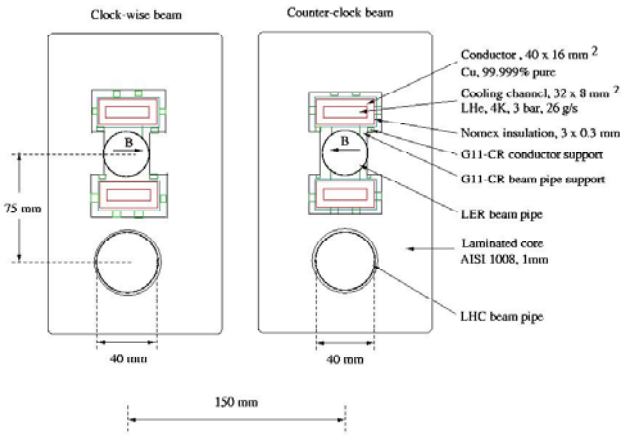

Figure 24. A pair of V6-type magnets with LHC beam pipes embedded in cores

As shown in Figure 25, the LHC beam pipes are well outside the core but for the first string of V7 magnets the LHC beam pipes may have to be inside the cryostat.

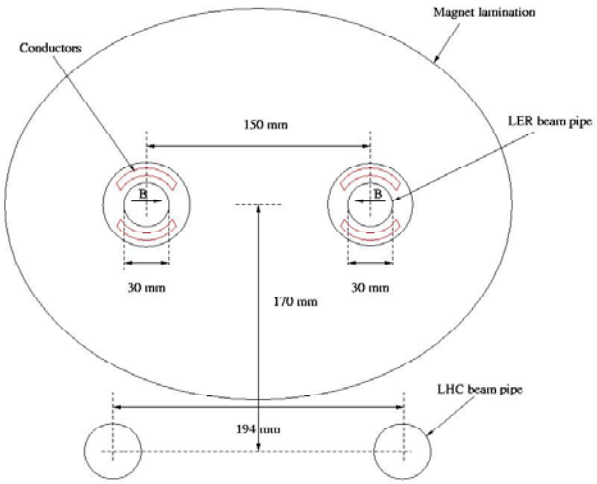

Figure 25. Conceptual arrangement of V7-type magnets at closest distance to LHC beam pipes

The new D1a and D1b are part of both LHC and LER. As discussed in detail in [2] these new D1 dipole magnets, with large apertures up to 140 mm, can be built to operate at a 8 T field using existing technology based on NbTi superconductors. In Figure 26 we illustrate the feasibility of such magnets using an analytical approximation of B_c (the central dipole field when the peak field is at the short sample limit) presented in [14].

The 8 T dipole, with an inner radius of 70 mm, is feasible using a 2-layer cable of 15 mm - 16 mm width and under the assumption of a reality factor of 85%. The feasibility of D1a and D1b from a mechanical and quench protection point of view is based on the experience with MFRESCA [15], a large aperture (88 mm bore) dipole operating at 10 T. As the projected magnetic force ratio of D1 is almost equal to the magnetic force in MFRESCA a similar mechanical design will be adequate. MFRESCA has only 60% of the projected stored energy of D1 at maximum field, but the energy density is very close because of the larger coil volume of D1. An adequate quench protection could be provided by using a fast quench detection system, with a large heater coverage (in order to spread the energy over the whole coil volume), and by a selecting large strand diameter (in order to reduce the inductance and therefore peak voltages).

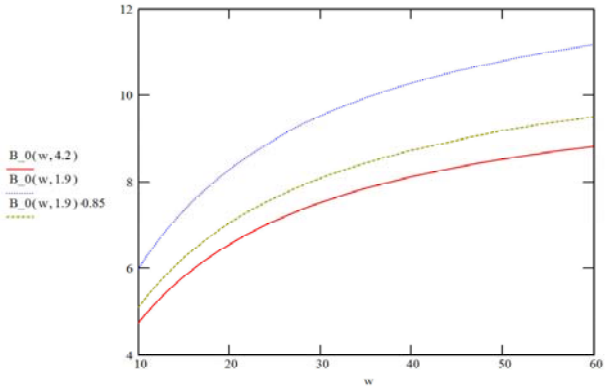

Figure 26. Projected central field (T) versus coil width (mm), when the peak field is at the short sample limit, at 4.2 K (red), at 1.9 K (blue), and at 1.9 K assuming 85% reality factor (green) for a large bore D1 dipole

5. THE LER RF SYSTEM

The LER accelerator must have its own RF system, so the acceleration of the LER beams can be performed independently of the status of the LHC. However, as shown in Chapter 7.2, the LER RF system requires twice the voltage of the LHC RF (32 MV/m versus 16 MV/m) if the LER beam losses caused by bunch coalescing should be kept down to an acceptable 5% level. Recently, the superconducting cavities operating at 35 MV/m - 40 MV/m fields, were successfully tested [16], and a strong development of high-field superconducting and normal conducting cavities is being vigorously pursued at present. For the symmetry with the LHC RF system the LER RF system should also be placed at IR4, but other locations, such as e.g. IR6, may also be considered. A possible arrangement of the LER RF system is shown in Figure 27. Although the two sets of LHC and LER cavities can certainly fit together in the IR4 space, adding there the LER RF associated power supplies may be very difficult. Consequently, one should plan for expanding the tunnel area including building alcoves, etc.. LER at IR4 will have its own set of dipole and quadrupole magnets facilitating proper horizontal clock-wise and counter-clock-wise beam separation

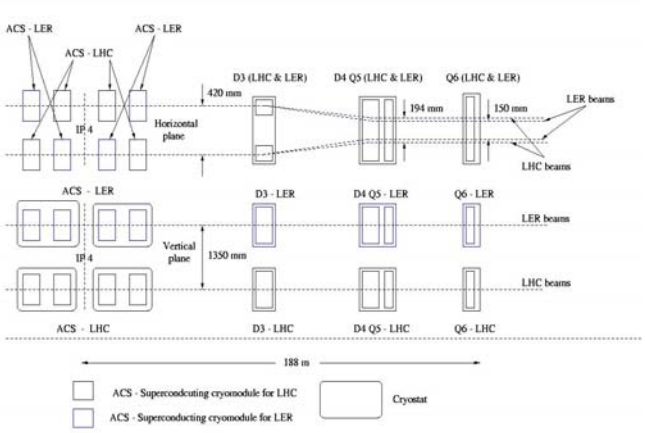

Figure 27. Possible arrangement of the LER RF system at IR4

6 THE LER LATTICE DESIGN

A preliminary optics for the LER is presented in [17]. The arc and dispersion suppresser cells were designed to replicate both the LHC optics and the accelerator footprint. The deduced parameters for the LER main arc magnets are shown in Table 5.

Table 5. Magnet parameters at 1.5 TeV in the arc and dispersion suppresser cells

Cell	Cell length [m]	Magnet length [m]	Number of magnets Per cell	B [T]	B' [T/m]
Arc	106.9	12.0	8	1.595	+/- 4.969
Dispersion suppresser	80.2	8.0	8	1.595	+/- 10.11

The B-fields and dimensions are smaller than the corresponding ones in the VLHC design [3], thus suggesting the possibility of an even higher field quality as well as facilitating easier fabrication and installation in the tunnel.As pointed-out earlier (Chapter 4.1), at IR1 and IR5 the LER and the LHC must share the LHC Q(1-3) triplets and first separation dipole D1. In the present LHC design the divergence of the beams exiting D1 is so gradual (1.11 mm/m) that the LER-LHC transfer line magnets can not be installed until just ~ 37 m from the face of D2. This distance is much to short to allow the LER beams to clear D2/Q4 magnet combo vertically. Consequently, the D1 dipole has to be replaced with a high-field, ~ 8 T, D1a magnet and at a 12.5 m distance, with an opposite polarity strong dipole (~ 8 T) D1b. Both LER and LHC beams require short D2 magnets to bring the horizontal separation of 150 mm for LER and 194 mm for the LHC. A list of LER-LHC transfer line magnets is shown in Table 4 (Chapter 4.2.3) and the list of the new D1 and D2 magnets is given in Table 6.

Table 6. Parameters of D1 and D2 dipoles for 1.5 TeV beams

Type	Magnet length [m]	B [T]	Beam path [m]	Altitude [mm]	Separation [mm]
D1a	8.96	1.70	8.96	0	27
D1b	7.70	1.70	29.13	0	130
D2-LER	1.00	2.14	52.63	75	150
D2-LHC	1.26	1.70	104.10	0	194

The LER lattice functions at IR1 and IR5 extending through the first full arc cell on each side of the straight section are illustrated in Figure 28. The LER optics is matched to the LHC injection $\beta^* = 18$ m, and β (max) = 400 m. The corresponding quadrupole parameters of the IR1 and IR5 straight sections for 1.5 TeV beams are listed in Table 7.

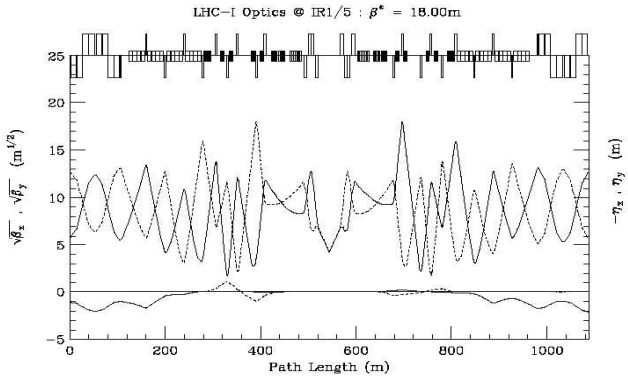

Figure 28. LER lattice functions at IR1 and IR5 straight sections.

Table 7. Straight section LER quadrupole parameters at IR1 &IR 5 for 1.5 TeV

Quad #	Length [m]	B' [T/m] u/s	B' [T/m] d/s
1	6.30	-40.847	40.847
2a&2b	5.50	40.847	-40.847
3	6.30	-40.847	40.847
4	2.0	131.09	-131.09
5	2.0	-157.03	157.03
6	2.0	198.65	-198.65
7	2.0	-143.52	143.52
8	2.0	159.34	-159.34
9	2.0	-66.78	66.78

There are two more quadrupoles in LER on each side of the IR than in the LHC. This is due to additional LER constraints of cancelling vertical dispersion and its derivative. The quadrupole # 9 is located directly above the LHC Q7.

7. LER ACCELERATOR PHYSICS ISSUES

7.1 The LER accelerator parameters and beam stability

The LER accelerator parameters are listed in Table 8. For comparison the parameters of the SPS are also presented as the LER is intended to replace the SPS as the main injector for the LHC. In addition the injection and extraction energies the main difference between the two machines is the size of the beam pipe as well as the average bunch current.

Table 8. LER vs SPS parameter set

Parameter	Units	LER	SPS
Inj./top energy	E inj/top, TeV	0.45/1.5	0.026/0.45
Circumference	C, km	26.659	6.916
Bunches/buckets	B, h_{RF}	2808/35640	288/4620
P/bunch	N_p, 10^9	115	115
Tune	Q	64.31/59.32	~26.6
Slip factor	S	0.00032	0.00186
Beta ave/max/min	β, m	66/182/31	~41
Beam pipe _ size	a/b, mm	14/21	22.5/70
Transverse emittance	ε_T , š μrad, rms	3.5	3.5
Current ave/bunch	I_B , mA/I_b , mA	580/0.2	230/0.8
RF frequency	F_{RF} , MHz	400	200/800
RF voltage (inj)	U_{RF} , MV	8	4/1
Synchrotron tune (inj)	Q_s	0.0031	0.0069
Bunch length (inj)	σ_s , cm, rms	13	110
Dp/p, rms (inj)	dp/p	0.0003	0.007

A comparison of the predicted LER instabilities versus those of the SPS is shown in Table 9. One can see that the TMCI and the space charge effects are considerably better with the LER. Also the LER resistive wall coupled bunch is improved as compared to the SPS one. The AC tune shift, however, must be improved e.g. by using a special AC quad, or via special loading. In summary, with special care the LER-LHC system may be able to handle twice the bunch current. The LER must use an Al beam pipe of a = 14 mm and coated with a 50 μm layer of copper or silver.

Table 9. Beam stability of LER versus SPS

	LER	SPS
TMCI e^9 N_{thr} / N_{nom}	770/115	260/115
Space-charge, dQ	0.0002	0.05
Res Wall, N_{turns}	~ 50	~ 70
AC tune e^{-3}, max/comp	24/2	3
E-cloud wrt SPS	~ 1	1
Long. Cpld. bunch/SPS	~ 1	1

Several methods are conceptually available to increase the beam intensity in the LER. These include bunch coalescing, momentum stacking and slip stacking. All of these processes are used in the FNAL injectors but only slip stacking seems practical in the LER. For example, bunch coalescing requires that the bunches which are to be coalesced should ideally be in adjacent buckets while the bunches in the LER will arrive with the nominal ten buckets spacing foreseen for the LHC bunches.

Momentum stacking requires a very large horizontal aperture so that bunches can be injected far off momentum.

Slip stacking is a process whereby two adjacent batches are combined to form a single batch of approximately twice the bunch intensity. In a collider the luminosity is given by:

$$L = \frac{f_{rev}}{4\pi\beta^* \varepsilon} M N_b^2 F(\varphi, \sigma_s)$$

where, f_{rev} is the revolution frequency, β* is the beta function at the IP, ε is the emittance, M is the number of bunches, N_b is the bunch intensity and F is a form factor which depends on the crossing angle ϕ and the bunch length σ_s. The luminosity is increased four-fold if the bunch intensity is doubled while keeping the same number of bunches. The expected luminosity increase will be slightly less since there will be losses during the slip stacking process. For example in the FNAL Main Injector, where slip stacking is part of everyday operations, losses are typically about 7%.

The slip stacking process to coalesce two adjacent bunches in the LER is shown schematically in Figure 29 by the RF frequency curves. After injection, the first batch is accelerated to an energy ΔE above the reference energy using a group of cavities tuned to a frequency f_{rf} - Δf_{rf} slightly below the reference RF frequency f_{rf}. This frequency difference Δf_{rf} is chosen so that the buckets for the two batches are well separated in energy. For our studies we chose $\Delta f_{rf} = 5\ f_s$, where f_s is the synchrotron frequency. This corresponds to an energy difference ΔE = 0.81 GeV at the injection energy 450 GeV.

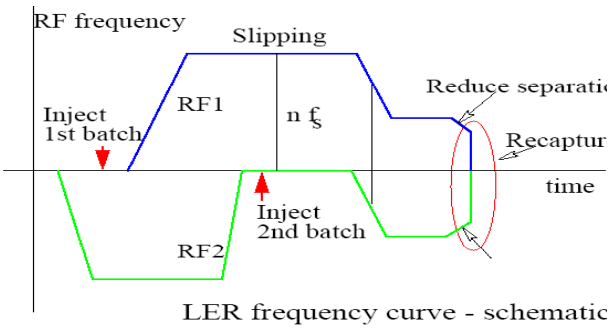

Figure 29. Schematic of a slip stacking process to capture 2 adjacent bunches

The second batch is injected on-momentum and both batches are then decelerated by an energy ΔE/2. This preserves their relative energy difference of ΔE. The batches are allowed to circulate in the ring for the time it takes for the lower energy batch to nearly catch up with the slower moving higher energy batch. The energy difference between the batches is decreased by changing the RF frequencies. At the moment that they are exactly aligned, they are captured in a single RF system at the reference frequency f_{rf}.

The energy difference just before recapture and the voltage of the RF capture system need to be chosen very carefully to minimize losses and emittance growth. Detailed simulations of the injection, slipping and capture process have been performed with the ESME code. These simulations show that emittance growth and beam loss during the slipping is negligible. The losses occur mainly during the final stages of reducing the energy difference and recapture. Figure 30 shows the net beam loss as a function of the capture voltage obtained after careful optimization.

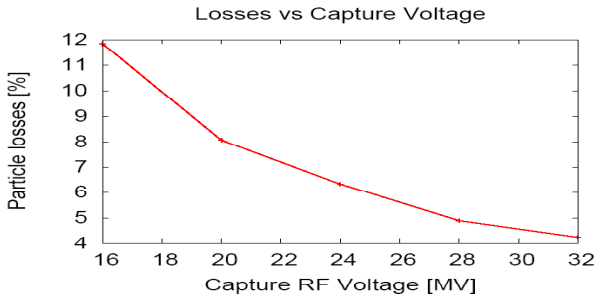

Figure 30. Beam losses versus capture RF voltage during batch recapture process

At 16 MV, the losses are about 12% and fall with voltage to around 4% at 32 MV. Increasing the voltage further does not significantly reduce the losses. The losses are then determined by the pre-capture stage. The drawback of higher capture voltages (besides cost and space) is that the longitudinal emittance of the captured bunch increases with the capture voltage as √V. Thus an RF capture voltage of 24 MV where the losses are about 6% might be sufficient.

Extraction from the LER can only be done once for each beam so all batches have to be coalesced at once. The batch length from the SPS will have to be adjusted so that the abort gap in the LER is at least as long as or slightly longer than the batch length. We assume that 12 SPS batches fill the LER. After the first set of 12 batches is injected, they are accelerated by ΔE. Then the next set of 12 batches is injected, one at a time into the LER abort gap. After both sets of 12 batches are injected, they are allowed to slip and then captured when they align as described above. Following the capture, these higher intensity bunches are accelerated to top energy and extracted to the LHC.

8. DETECTOR AND ACCELERATOR COMPONENT SAFETY WITH LER

8.1 The LER beam dump system

The LER accelerator will use its own beam dumps systems. They will be located in IR6 where also the LHC beam dumps are situated. As the LER ring is 1.35 m above the LHC ring, the beam dump magnetic

components will not interfere with the LHC ones, as indicated in Figure 31.

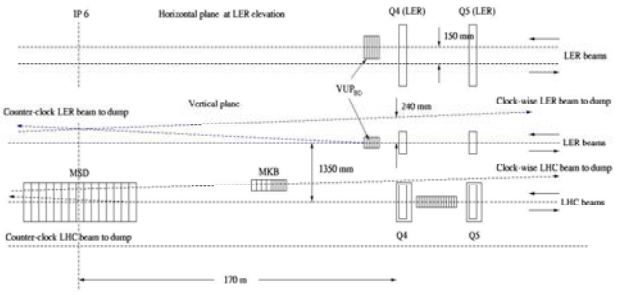

Figure 31. Conceptual arrangement of the LER beam dump system for the counter-clock beam

The LER beams will be dumped into the upper level tunnel locations on both sides of the IR6. The magnetic bending power to send the LER beams into a dump is considerably smaller than that for the LHC beams due the 5 times lower energy and the fact that the LER ring is already at very high elevation as compared to the LHC.

8.2 The LER pilot beam bunches

The CERN PS is able to inject a single low intensity bunch into the SPS, which after ramping to an energy of 0.45 TeV is then injected to the LHC (pilot bunch). This allows testing of the LHC readiness to accept the high intensity beam at 0.45 TeV. The 0.45 TeV beam stacking in both LHC rings takes about 20 minutes, after which time the LHC magnets are ramped to 7 TeV. With the LER injector the beam stacking takes place in the LER rings instead of the LHC ones. Consequently, the single PS/SPS pilot bunch that is now injected to the LHC can be injected to the LER, and then used for testing the common LER and LHC accelerator systems in a "pre-stacking" time period.

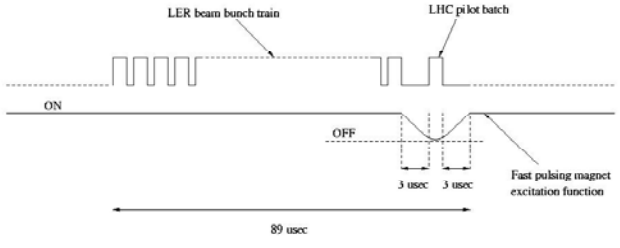

Figure 32. The LER beam bunch train and the excitation function of the LER-LHC transfer line magnets to transfer a pilot beam batch to LHC

The stacked beam bunch train in the LER will also contain a short (e.g. 1 μsec long) beam batch separated by 3 μsec gaps on both sides. As shown in Figure 32, by using a sine-wave function for the excitation of the fast switching LER-LHC transfer line magnets it will be possible to inject this beam batch as the LHC pilot beam to test the LHC at the 1.5 TeV level, before the transfer of a full intensity of the stacked LER beam to the LHC is enforced.

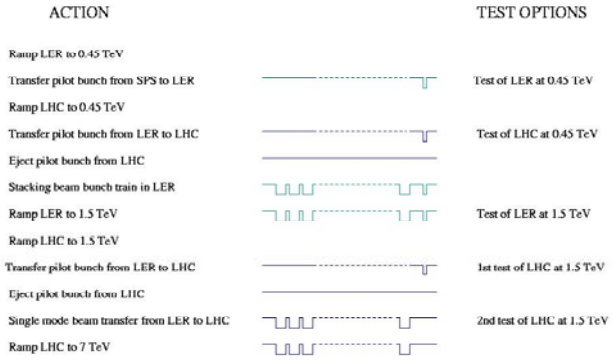

Figure 33. Possible sequence of pilot beam transfers for testing the LER and LHC

8.3 Detector and accelerator emergency protection from a failed LER beam

In the situation of a major catastrophic failure of the LER accelerator components e.g. just before transferring the 1.5 TeV beams into the LHC, and with a danger that large portion of the beam could not be extracted in time into the IR6 beam dump, one may resort to a localized LER beam dump system. Such local beam dumping systems can only be placed in the accelerator straight sections. One of possible locations is the LER beam drift space at IR1 and IR 5 between the LER Q5 and Q6 (equivalent to the LHC ones) as shown in Figure 34.

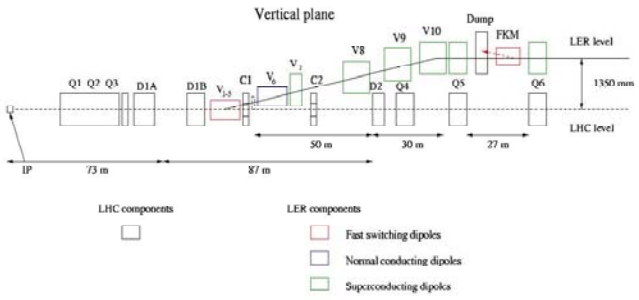

Figure 34. Conceptual arrangement of a local beam dump for the counter-clock LER beam

This beam dump will consist of a fast kicker magnet string (FKM) and a beam absorber. The FKM magnet string has to lift the LER beam by at least 25 mm to be 10 mm above the LER beam pipe before entering the dump. With a FKM magnet B-field of 1.5 T, a 13 m long string of magnets will lift the 1.5 TeV beam by 28 mm, and a beam dump of 5 m length is sufficient to stop the beam and to contain a large part of the induced radiation. The total length of the beam dump system is then ~ 18 m,

much less than the available space of 27 m between the Q5 and Q6. The FKM magnetic field will have the rise-time of 3 μs, and its flat top will have to last for at least half of the LER beam circulation time, or 45 μs.

These local beam dump systems at IR1 and IR5 provide an important improvement of the protection not only for the detectors but also for the LHC and LER components in those areas. Any malfunctioning of the LER transfer line magnets can trigger the powering of the FKM magnets. As these magnets are very close to the LER-LHC transfer line, the only delay in beam dumping is their rise time of 3 μs. This means that at most 1/30 (3 μs / 89 μs) of the failed LER beam will potentially scatter into the transfer line magnets.

The Q1,2,3 magnets are the ones most exposed to radiation caused by a failed LER beam in the area of the fast switching magnets. In the vertical plane the FSM's are transporting the LER beam between 0 mm and 45 mm separation from the LHC nominal beam path. As these magnets are nearly 90 m away from the interaction region their total failure will send beams undisturbed through the large bore HD1b and HD1a LHC dipoles, and then into the absorbers placed in front of the Q1,2,3 triplet, as indicated in Figure 35. The situation is more subtle, however, when only the FSM magnet closest to the HD1b dipole fails. In this case there is a possibility that portion of the beam will be scraping the collimator, and then it may also be scraping the beam pipe inside the Q1,2,3 triplet. A detailed study of the failed beam trace is needed to evaluate the level of danger to the Q1,2,3 magnets as well as to the detector itself arising from such a situation. One way to reduce the effect of the beam scraping inside the LHC beam pipe is to dilute the beam energy density while the beam is still scraping the beam pipe within the FSM magnet string. The dilution can be achieved with a help of the carbon scatter block placed inside these magnets as shown in Figure 36.

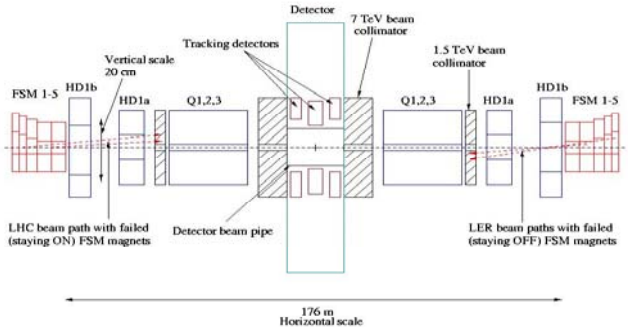

Figure 35. Possible arrangement of collimators for the FSM magnets string

The carbon scatter block is about 1 cm thick, and it covers the entire length of the beam pipe in the FSM magnet string. For the counter-clock beam the scatter block is below the beam pipe (as shown in Figure 35), and for the clock-wise beam it will be above the beam pipe. The introduction of the scatter block widens the magnet vertical width. This does not affect the current strength required for a given B-field, but it does increase the magnet inductance, and so the peak voltage value during the turn-on or turn-off operation is also slightly increased.

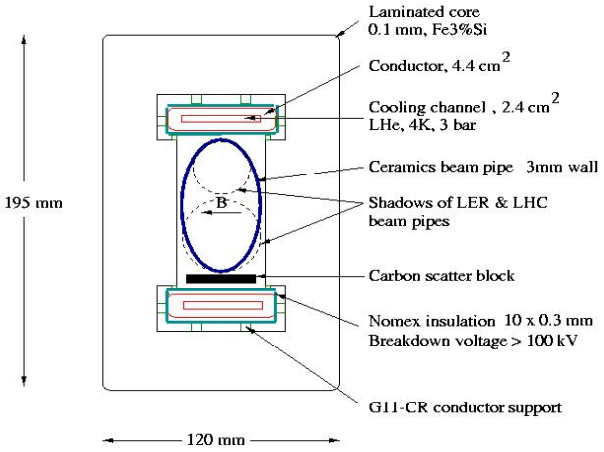

Figure 36. A conceptual arrangement of a carbon scatter block inside the FSM magnet.

9. MAJOR LER COMPONENT COST, FABRICATION AND INSTALLATION SCHEDULE

9.1 Major LER component list and cost estimate

The cost in 2006 $ was estimated by scaling down by a factor of 10 from the VLHC proposal [1], and then applying the current price of the raw materials. The cost of the power supply systems, cooling water, etc. is included in the cost of the components.

Table 10 LER cost estimate

	System	**[$M]**
1	Main arc magnets	64
2	Arc corrector magnets	4
3	Fast switching magnets	28
4	Other transfer line magnets, including D1	14
5	Beam dump magnets (at IR4, IR1 and IR5)	12
6	RF system	10
7	Beam pipe vacuum system	16
8	Cryogenic system (excluding cryoplant)	8
	Grand total	**156**

The cost of the magnet support fixtures in the tunnel, and the cost of some necessary modifications (e.g. possible need for enlargement of the tunnel height/width at the transfer line locations as well as alcoves at IR4 for the LER RF system electronics) are not included in the above cost estimate.

9.2 Schedule for LER component fabrication and installation in the LHC tunnel

A task flow-chart is shown in Figure 37, and the very tentative schedule (see Table 11) is very speculative.

Table 11 Tentative schedule

	Activity	Time [Y]	Lapsed time [Y]
1	LER accelerator design, including transfer lines	1	1
2	Prototyping and testing transfer line magnets (and main arc dipole magnet, if needed)	2	2
3	Preparation of main arc magnet industrial production	1	2
4	Magnet production	3	5
5	Magnet installation in the tunnel	2	5
6	LER commissioning	1	6

Items 1–3 and the items 4-5 can proceed simultaneously, but item 4 must follow items 1-2, so the magnet production cannot start sooner than 2 years from the time "zero". As soon as some arc magnets are produced and tested, the installation in the LHC tunnel may begin. The overall lapsed time for the LER completion work will be determined, however, by the number of months per year allowed for LER installation, and the number of crews working simultaneously on the installation in the tunnel. We assumed that 20 crews of 6 people should be able to install 40 magnets per week, or 1200 magnets in 30 weeks (~ 8 months). Hence with one 4-months break of the LHC operation per year, the LER installation in the tunnel may be completed in a period of two years. In summary, the LHC operation with the LER as injector could be ready in 6 years from time "zero".

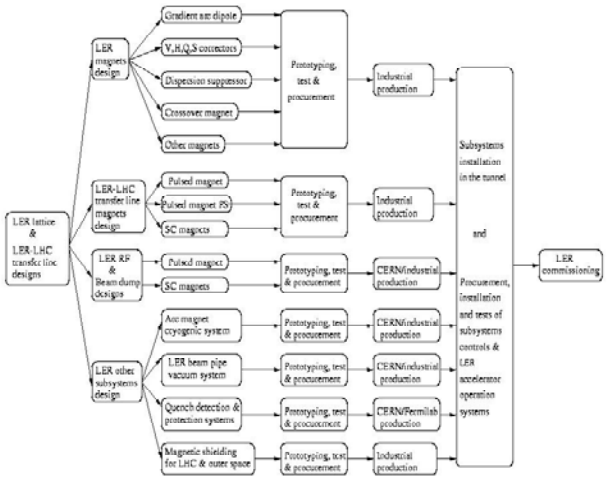

Figure 37. A task flow-chart for LER accelerator design and construction based in part on VLHC Stage 1 construction schedule proposal [3].

10. APPLYING THE LER MAGNET TECHNOLOGY TO A FAST CYCLING SPS

One can consider an application of the LER magnet technology described above in other type of accelerators. Below we describe briefly a proposal for a fast cycling SPS (SF-SPS, Super-Ferric SPS) at CERN. The main characteristic of the LER (or the VLHC Stage 1) accelerator is that it consists of a string of magnets energized by a common conductor (e.g. transmission-line type) with one common power supply connected to the magnet string via one set of high-power current leads, as shown earlier in Figure 6. This arrangement simplifies the accelerator structure as well as its operation, and in the process helps to significantly reduce the overall cost.

In the VLHC and LER designs, the magnetic core determines the strength of the B-field in the magnet gap. A field of 2 T is a practical limit where saturation effects can be suppressed to an acceptable level. With a 2 T field the SF-SPS can be designed to accelerate beams to 500 GeV. The layout of the PS-SPS-LHC accelerator complex is shown in Figure 38.

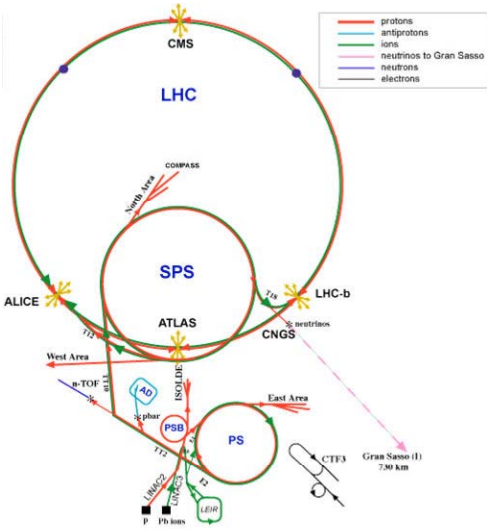

Figure 38. The layout of the CERN accelerator complex

One can see that the proton beams in the PS and the SPS circulate in only one direction. This implies using magnets with beam gaps where their B-fields are oriented in the same direction. This requirement does not allow application of the VLHC-type magnetic design as the field in the gaps is of opposite direction, but the fast switching magnet design proposed for the LHC-LER transfer lines can be adapted to the SF-SPS (and the PS for that matter). As the energy of the beams in PS and SPS is low, the beam pipe size is rather large (40 mm high and 70 mm wide) and so the magnet gap has to be no less than 40 mm. This implies using a conductor current in the range of 100 kA for a 2 T field. If we limit ourselves to this maximum current value than there have to be two independent magnet rings for the SF-SPS two-beam accelerator. A possible arrangement of such a set of magnets is shown in Figure 39.

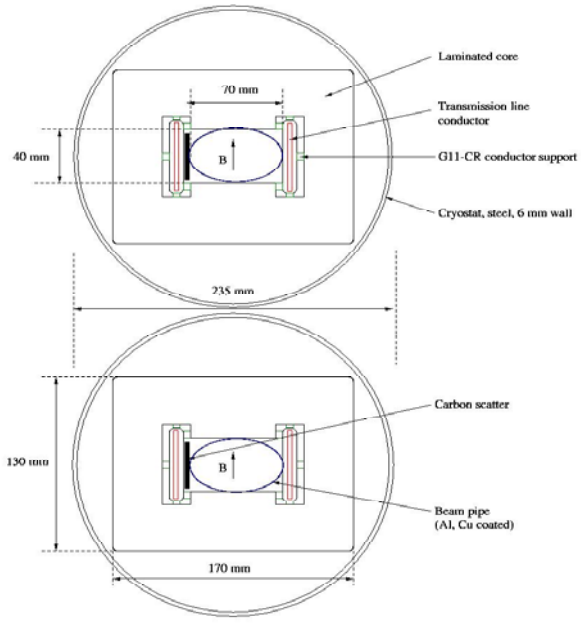

Figure 39. Arrangement of a two-dipole magnet set for the SF-SPS.

One can easily see that it is also possible to have 2 sets of the C-type magnets sitting side by side, and then using only one conductor loop to generate the B-field in both magnet gaps. This arrangement is shown in Figure 40. Although there is only one conductor loop in the second case the number of conductor strands is doubled of that in the first case as the current to power the magnet for the same B-field has to be doubled. Consequently, there is no saving in the conductor amount. In addition, the magnetic design of the C-type magnets is considerably more difficult, especially in the B-field range close to the saturation.

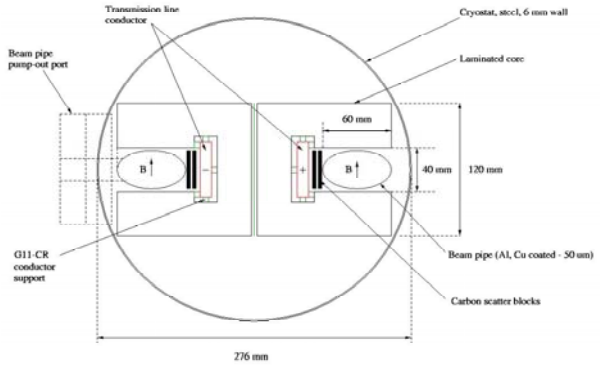

Figure 40. Possible arrangement of C-type magnets for 2 beam SF-SPS accelerator

The only gain is in the mechanical simplification as both magnets are placed inside the common cryostat. In both type of magnets we installed carbon scatter blocks to protect the conductors from failed beams. In designing fast switching magnets we followed the principles of the transmission line super-ferric magnet design, except for changing the structure of the superconductor, and limiting the magnet string length to a few meters in order to minimize the inductance, and in this way to help accommodating the power supply fast switching-off operation.

With accelerator cycling time of 1 s - 3 s, the magnet string can be very long, and as it turns-out even equal to the accelerator circumference in case of the SF-SPS. The inductance for the magnets in Figure 36 is estimated to be ~ 3 μH per meter. The inductance of the one entire SF-SPS accelerator ring is then ~ 20 mH, and the voltage drop/rise for 1 Hz operation at 90 kA current is ~ 1.6 kV, a very manageable value. The key then to the successful SF-SPS operation is the level of the tolerable Eddie current induced B-fields, both in the conductor and the magnet lamination. As these magnets must continually cycle there is no time for recovery (except of a short flat top, 10 ms - 100 ms to stabilize and then extract beams), and so each newly injected beam must meet the proper magnetic field. In Table 12 we summarize preliminary assessment of the Eddie current B-fields for the NbTi and HTS(344S) conductors, as well as for the Fe3%Si laminations of 1mm and 100 μm thickness, respectively. These predictions are for 0.33 Hz and 1 Hz magnetic field cycling operations.

Table12. Projected Eddie current B-fields for the SF-SPS magnets

Conductor or lamination	**f = 0.33 Hz**	**f = 1 Hz**
NbTi, 0.42 mm^2	4 mT	7 mT
HTS (344S), 0.65 mm^2	0.05 mT	0.09 mT
Fe3%Si, 1000 μm	17 mT	30 mT
Fe3%Si, 100 μm	1.7 mT	3 mT

The conclusion from the above table is that using a HTS(344S) superconductor is superior to a NbTi one. One should also note that during ramping up the induced Eddie B-field has the opposite sign to that generated in the followed-up ramping down. This may help to keep the "average" magnet B-field at the proper value. Careful simulations of the beam transport and acceleration in the SF-SPS must be done to find out what are the acceptable limits for the induced Eddie current B-fields. If necessary the magnetic core can be made of 50 μm thick, Fe3%Si lamination, thus lowering the Eddie current B-field in the laminations to a value below 1 mT for the 3 s cycle type of the SF-SPS operation.

The use of a superconducting line to energize the SF-SPS magnets strongly suppresses the required cryogenic support. The heat load for the SF-SPS conductor should be in the same range as for the LER main arc magnets. For two accelerator rings of ~ 7000 m each, the projected heat load is then ~ 2.1 kW at a 4.5 K - 6.0 K level, and ~ 42.5 kW at a 50 K - 75 K level, which is about 1/10 of

the one LHC cryo-plant power. Consequently, the cryogenic demands of the SF SPS could be supported from the existing LHC cryogenic system, especially that the SF-SPS operations will not likely overlap in time with those of the LHC.

The estimated cost (by scaling from the LER) for the SF-SPS accelerator based on a NbTi conductor is ~ $ M100, and based on a HTS (344S) conductor at 2006 price doubles to ~ $M 200, but possibly only $M 120 if the HTS(344S) conductor price drops by a factor of 5 in 2008, as indicated by the American Superconductor Corporations [11].

11. CONCLUSIONS

We made a preliminary assessment of the feasibility for installing an injector accelerator ring (LER) in the LHC tunnel using the VLHC Stage 1 transmission line magnets. We believe that there are no serious obstacles in principle for such an undertaking. The transfer of the beam from the LER ring to the LHC one is challenging, but it seems feasible. A re-arrangement and re-design of the D1 LHC dipole is however needed, to facilitate the installation of the LER-LHC transfer line. A preliminary cost analysis of the LER suggests that it is below the LHC yearly operational expenditure and thus very much affordable. In addition, the LER components can be manufactured and then installed in the LHC tunnel during the regular LHC shut-downs in a reasonable time span of 5-6 years without interference with the ongoing LHC physics program in the same time period.

With a second accelerator in the LHC tunnel the complexity of the overall LHC system is significantly increased raising concerns about the detector and accelerator components safety. A limited use of pilot bunches provided by the SPS is possible and may potentially improve the safety of the LHC-LER complex. In addition, installation of dedicated kicker magnets and beam dumps in the straight sections (especially in the IR1 and IR5 ones to protect detectors) will allow for a safe removal of the LER beams from the circulation in case of a catastrophic failure of the transfer line magnet system (or other significant LER component) when a standard beam dumping at IR4 may not be sufficiently effective. The radiation implications of such a system still have to be evaluated.

A feasibility study of bunch slip stacking in the LER suggests the possibility of a luminosity increase of up to a factor of 4. The combination of this luminosity increase with a potential improvement of the LHC beam transport and acceleration due to the increased injection energy to 1.5 TeV may lead to the overall LHC luminosity increase in an order of magnitude. Such an improvement of the LHC performance would greatly facilitate the working of the detectors allowing for a significant increase in streaming of the hard-collision data relative to the multiple interaction backgrounds. In this way the boundaries of the LHC physics reach will be expanded much beyond the present expectations. In a longer term the implementation of the LER will provide a very strong boost to the LHC energy upgrade proposal (DLHC).

It appears that the magnet technology developed for the VLHC combined with the one for the proposed fast switching magnets of the LER also offers a new option for an SPS application allowing it to become a fast cycling accelerator while not being used for the injection of beams to the LHC. This would enhance prospects for the fixed target physics at CERN, especially neutrino physics, which requires proton beams of a very high integrated intensity. It would only be natural to extend the proposed fast cycling magnet technology to the PS, upgrading its beam energy to 50 GeV in the same time. The proposed fast switching/cycling magnet technology, however, needs a vigorous R&D effort to prove expectation of the performance, and to prove its high cost-effectiveness.

ACKNOWLEDGEMENTS

We greatly profited from several illuminating discussions with Gianluigi Arduini, Jean-Pierre Koutchouk, Yvon Muttoni, John Osborne, Germana Riddone of CERN, with William Foster, Vladimir Kashikhin of Fermilab, and with Masayoshi Wake of KEK.

We are also greatly indebted to Steve Holmes, Robert Kephart, Peter Limon and Steve Peggs for their inspiration and support.

REFERENCES

[1] LHC Design Report Vol 1, O. Brunning et al., CERN-2004-003, Section 4.7 Dynamic aperture

[2] G. de Rijk, L. Rossi and H. Piekarz, Preliminary Study of Using “Pipetron”-type Magnets for a Pre-accelerator for the LHC”, EPAC, Scotland, 2006

[3] Design Study for a Staged VLHC, Fermilab-TM-2149, 2001

[4] H. Piekarz, Test of 2 Tesla Superconducting Transmission Line Magnet System, MT19, Genoa, 2005

[5] S. Hays, The 100 kA DC Power Supply for a Staged Hadron Collider Superferric Magnet, MT19, Genoa, 2005

[6] Y. Huang, The 100 kA Current Leads for Superconducting Transmission Line Magnet, MT19, Genoa, 2005

[7] Vl. Kashikhin, Test Results of a 2 Tesla Transmission Line Magnet obtained with 102 Sensor Array of Hall Station, MT19, Genoa, 2005

[8] G. Velev, Field Quality Measurements of a 2 Tesla Transmission Line Magnet, MT19, Genoa, 2005

[9] H. Piekarz and G.W. Foster, Design Study for VLHC, Sec. 5.2.4, Fermilab-TM-2149, 2001 (unpublished)

[10] S. Hays, A 5 Megawatt Ramping Power Supply for the Fermilab Main Injector Dipole Bus, IEEE

Conference, Nuclear Science Symposium, Volume 1, p. 390-393, 1993
[11] Garry Fergusson, American Superconductor Corp., Devens, MA 01432 (2006)
[12] M. Mayer, D. Fox, F. Castronuovo and U. Jansson, IEEE Transactions on Magnetics, Vol. 40, No. 4, 2004 (page 3051)
[13] T. Isono, K. Hamada and K. Okuno, Cryogenics 46 (2006) 683-687
[14] E. Todesco and L. Rossi, to be published in Proc. of WAMDO, April 2, 2006
[15] D. Leroy, et al., Design and Manufacture of a Large Bore, 10 T, Superconducting Dipole for the CERN Cable Test Facility, IEEE Transactions on Applied Superconductivity, Vol. 10, No 1, March 2000
[16] L. Lilje et al. NI&M vol. 524, issue 1-3, p.1-12, 21 May, 2004
[17] J. Johnstone, "Optics of a 1.5 TeV Injector for the LHC", EPAC, Scotland, 2006